Title	Investigation of mechanical properties of stress-relieved and electron-irradiated tungsten after hydrogen charging
Author(s)	Sato, K.; Yamashita, H.; Hirosako, A.; Komazaki, S.; Xu, Q.; Onoue, M.; Kasada, R.; Yabuuchi, K.; Kimura, A.
Citation	Nuclear Materials and Energy (2018), 17: 29-33
Issue Date	2018-12
URL	http://hdl.handle.net/2433/235017
Right	© 2018 The Authors. Published by Elsevier Ltd. This is an open access article under the CC BY-NC-ND license (http://creativecommons.org/licenses/BY-NC-ND/4.0/).
Type	Journal Article
Textversion	publisher

Nuclear Materials and Energy 17 (2018) 29–33

Contents lists available at ScienceDirect

Nuclear Materials and Energy

journal homepage: www.elsevier.com/locate/nme

Investigation of mechanical properties of stress-relieved and electron-irradiated tungsten after hydrogen charging

K. Sato[a,*], H. Yamashita[a], A. Hirosako[a], S. Komazaki[a], Q. Xu[b], M. Onoue[c], R. Kasada[d], K. Yabuuchi[e], A. Kimura[e]

[a] Graduate School of Science and Engineering, Kagoshima University, Kagoshima-shi, Kagoshima 890-0065, Japan
[b] Research Reactor Institute, Kyoto University, Kumatori-cho, Sennan-gun, Osaka 590-0494, Japan
[c] Natural Science Center for Research and Education, Kagoshima University, Korimoto, Kagoshima 890-0065, Japan
[d] Institute for Materials Research, Tohoku University, Sendai-shi, Miyagi 980-8577, Japan
[e] Institute of Advanced Energy, Kyoto University, Uji-shi, Kyoto 611-0011, Japan

ARTICLE INFO

Keywords:
Tungsten
Hydrogen
Hardness
Tensile test
Defects
Electron irradiation

ABSTRACT

The effect of hydrogen on the hardness and tensile properties of pure tungsten was examined using Vickers hardness and tensile tests. Samples were exposed to high-pressure hydrogen gas (5.8 MPa). The tensile behavior, tensile fracture surface, and hardness of as-received and stress-relieved tungsten did not change after hydrogen charging, owing to the low solubility of hydrogen. Therefore, to understand the effect of hydrogen on these materials, experiments must be performed to trap more hydrogen atoms at dislocations. In contrast, the hardness of electron-irradiated tungsten increased after hydrogen charging. Additionally, after a heat treatment at 473 K, hydrogen atoms dissociated from single vacancies, and the hardness decreased to the pre-charged value. Thus, single vacancies decorated with hydrogen atoms are expected to obstruct dislocation motion.

1. Introduction

In a fusion reactor, plasma-facing materials (PFMs) must withstand the damage caused by plasma-borne neutrons [1], hydrogen atoms [2], helium atoms [3] and heat loads [4]. Therefore, a high melting point, high thermal conductivity, and low sputtering erosion are required for PFMs. High-Z materials such as tungsten have been employed as PFMs owing to their thermal properties and resistance to erosion [5,6]. Additionally, hydrogen isotopes penetrate PFMs upon exposure to a fusion plasma [7]. Irradiation-induced defects capture the hydrogen isotopes, which are retained by the materials [8–10]. In tungsten, hydrogen solubility is very low, and defects bind to hydrogen atoms very strongly [11]. For example, Ogorodnikova et al. reported that the binding energies of deuterium to dislocations, vacancies, vacancy clusters, and voids were 0.46 eV [12], 1.06 eV [13], 1.06 eV [14], and 1.4 − 1.9 eV [13,15,16], respectively. Therefore, it is especially important to investigate the interaction between hydrogen and tungsten defects.

The retention of hydrogen isotopes typically degrades the mechanical properties of materials, causing effects such as hydrogen embrittlement [17,18]. If tungsten is widely used for fusion reactor components, hydrogen embrittlement of tungsten as structural materials may become critical. Several mechanisms of hydrogen embrittlement, for example, hydrogen-enhanced localized plasticity [19], hydrogen-enhanced decohesion [20], and the hydrogen-enhanced, strain-induced vacancy model [21] have been suggested, but a detailed description of the mechanism has not yet been identified. By molecular dynamics simulations, Yu et al. showed that hydrogen atoms promote the motion of dislocations in tungsten [22]. Terentyev et al. investigated the surface hardness of tungsten exposed to high-flux deuterium plasma by nanoindentation [23]. Plasma-induced defects were demonstrated to obstruct the motion of dislocations. In this study, hydrogen atoms were charged on electron-irradiated and stress-relieved tungsten, and their effect on the hardness and tensile behavior of tungsten was studied to clarify the mechanism of hydrogen embrittlement.

2. Experimental procedure

High-purity tungsten samples (99.95%, A.L.M.T. Corp.) were used in this study, and Fig. 1 shows the shape of the samples used in the tensile tests. Samples for tensile tests were cut from a 0.1-mm-thick sheet using a wire electric discharge machine. To release stress, the tungsten was annealed under two different conditions (at 1173 K for 1 h and at 1273 K for 5 h under vacuum ($<10^{-4}$ Pa)). For the electron irradiation tests, 5-mm-diameter samples were cut from a 0.2-mm-thick

* Corresponding author.
E-mail address: ksato@mech.kagoshima-u.ac.jp (K. Sato).

https://doi.org/10.1016/j.nme.2018.08.003
Received 15 December 2017; Received in revised form 19 July 2018; Accepted 11 August 2018

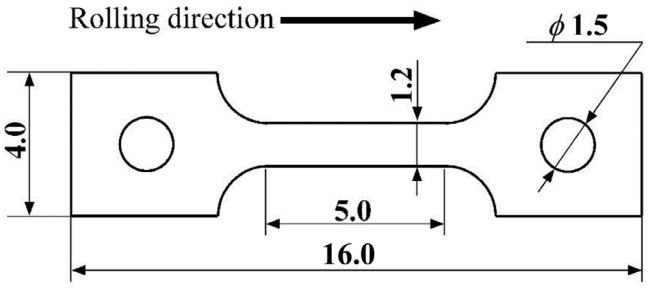

Fig. 1. Shape of samples for tensile tests. Thickness was 0.1 mm.

sheet using a wire electric discharge machine. Then, they were annealed at 1773 K for 1 h in vacuum ($<10^{-4}$ Pa) to allow recrystallization. Electron irradiation was performed using the electron linear accelerator of the Research Reactor Institute at Kyoto University. The electron acceleration voltage was 8 MV. The irradiation doses were 1.4×10^{21}, 4.2×10^{21}, 1.4×10^{22}, 3.0×10^{22}, and 6.5×10^{22}/m^2 (1.4×10^{-5}, 3.8×10^{-5}, 1.4×10^{-4}, 2.9×10^{-4}, 6.4×10^{-4} dpa). To calculate doses, an atomic displacement cross-section of 70.4 barns and a displacement threshold energy of 84 eV were used [24]. The irradiation temperature was 363 ± 10 K, which was maintained with water cooling. All samples were electropolished after electron irradiation to remove the oxidized layers formed during water cooling.

The hydrogen atoms were charged to the samples by exposing them to hydrogen gas at a pressure of 5.8 MPa and a temperature of 573 K for 240 h. Under these conditions, the hydrogen concentration of tungsten according to Sieverts' law is 1.12×10^{-11}, which is so low that hydrogen bubbles or platelets are not formed. Before hydrogen charging, the electron-irradiated samples were annealed at 573 K for 240 h in a vacuum to prevent the formation of vacancy clusters during hydrogen charging. The microscopic Vickers hardness $Hv_{0.1}$ was measured at 298 K with a load of 0.1 kg•f using a HMV-2T (Shimadzu Corp.), applied for 10 s. The average values and standard deviations of the hardness in 10 tests are plotted below. Different machines with the same model number were used for the hardness tests discussed in Sections 3.1 and 3.2. Tensile tests were performed at 298 K with a strain rate of 2.9×10^{-4}/s and a 500 N load cell. The tensile test machine was manufactured by INTESCO Co., Ltd. Results of the tensile tests of recrystallized and electron-irradiated tungsten were not obtained because the samples were broken while affixing them to jigs. Hydrogen-charged samples were cooled with liquid nitrogen unless otherwise specified in the description of the experimental tests above.

3. Results and discussion

3.1. As-received and stress-relieved tungsten

Fig. 2 shows the stress–strain curves in as-received and stress-relieved tungsten. Table 1 gives the 0.2% proof stress and tensile strength of as-received and stress-relieved tungsten with and without hydrogen charging. The 0.2% proof stress and tensile strength decreased with increasing annealing temperature during stress release. Both also slightly decreased after hydrogen charging in all samples, but the change was negligible. Therefore, it was unlikely that the observed change was due to hydrogen charging.

Fig. 3 shows the change in Vickers hardness in as-received, stress-relieved, and recrystallized tungsten before and after hydrogen charging. The Vickers hardness of the recrystallized tungsten was higher than that obtained in a previous study [25]. The tensile strength and Vickers hardness of the recrystallized tungsten have been reported to be 1070 MPa and 380 kgf/mm^2, respectively [25]. The application of a heat treatment at 1773 K for 1 h here was not sufficient to obtain perfect recrystallization. The hardness decreased as the annealing temperature increased during stress release. Fig. 4 shows SEM images of the

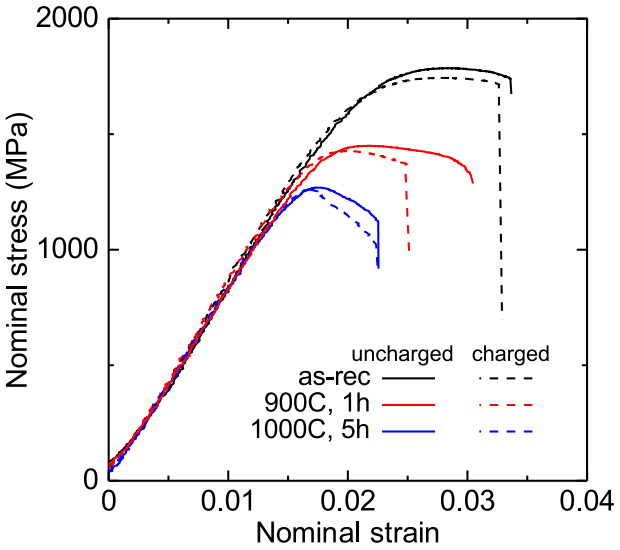

Fig. 2. Stress–strain curves of as-received and stress-relieved tungsten. Stress release was performed at 1173 K for 1 h and at 1273 K for 5 h.

Table 1
0.2% proof stress ($\sigma_{0.2}$), tensile strength (σ_{TS}) of as-received, and stress-relieved tungsten with and without hydrogen charging. Stress release was carried out at 1173 K for 1 h and at 1273 K for 5 h.

		Non-charged		Hydrogen charged	
		$\sigma_{0.2}$ (MPa)	σ_{TS} (MPa)	$\sigma_{0.2}$ (MPa)	σ_{TS} (MPa)
As-received		1677	1786	1659	1744
Stress relieved	1173 K, 1 h	1418	1450	1407	1427
	1273 K, 5 h	1264	1269	1258	1261

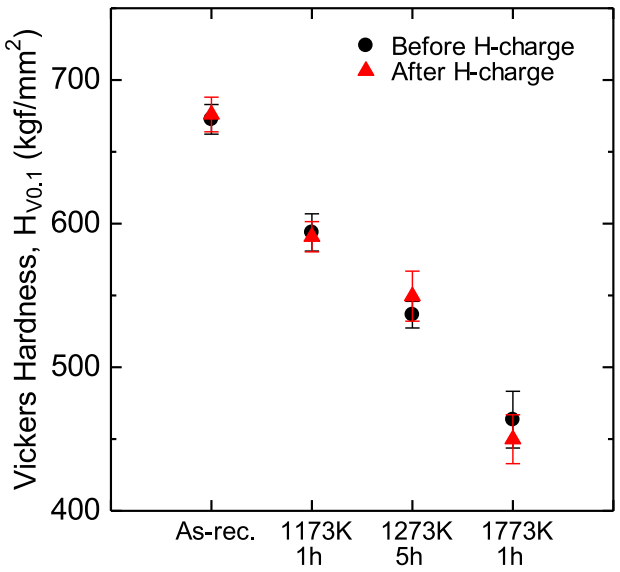

Fig. 3. Change in Vickers hardness in as-received, stress-relieved, and recrystallized tungsten after hydrogen charging.

surface of as-received tungsten, tungsten annealed at 1173 K for 1 h, tungsten annealed at 1273 K for 5 h, and tungsten annealed at 1773 K for 1 h after hydrogen charging. SEM observations were not performed before hydrogen charging; however, the same sample was used for hardness tests before and after hydrogen charging. The grain size did not change with increasing annealing temperature up to 1273 K, and substantially increased after the annealing at 1773 K. These results

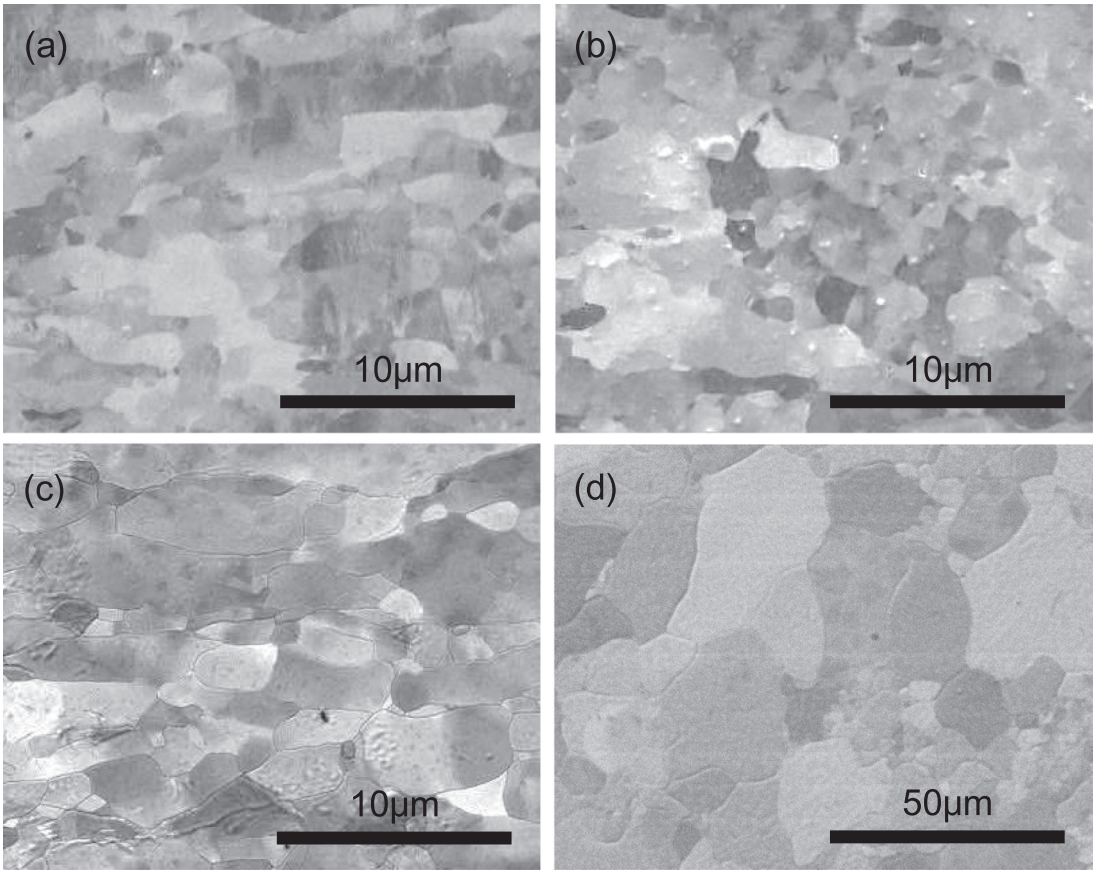

Fig. 4. SEM images of the surface of (a) as-received tungsten, (b) tungsten annealed at 1173 K for 1 h, (c) tungsten annealed at 1273 K for 5 h, and (d) tungsten annealed at 1773 K for 1 h after hydrogen charging.

indicate that the hardness and tensile strength mainly depend on the density of residual dislocations in the annealing below 1273 K, and depend on dislocation density and grain size after annealing at 1773 K. The hardness was nearly constant before and after hydrogen charging. The concentration of hydrogen atoms trapped at dislocation cores was analyzed based on a theoretical model similar to that in [26], and the concentration in this study was not sufficient to either promote or suppress dislocation motion (e.g., softening effect of hydrogen atoms [22]). When the dislocation density, hydrogen solubility, and temperature are controlled, additional hydrogen atoms can be trapped at dislocation cores, enabling the detection of how hydrogen affects dislocation motion.

3.2. Electron-irradiated tungsten

Fig. 5 shows the change in Vickers hardness of electron-irradiated tungsten versus irradiation dose. Fig. 6 shows SEM images of the surface of (a) tungsten annealed at 1773 K for 1 h used in Section 3.2, and (b) tungsten irradiated with electrons at doses of 6.4×10^{-5} dpa. The grain size was not significantly different between the samples mentioned in Sections 3.1 and 3.2. Therefore, the hardness difference of recrystallized tungsten between that discussed in Section 3.1 ($Hv_{0.1}$ = 464 kgf/mm^2) and here ($Hv_{0.1}$ = 414 kgf/mm^2) was caused by the different machines used in each section or material organization except for grain size, which should be investigated in the future. Since the time for electropolishing the electron-irradiated samples was longer than that for the unirradiated samples, their surface textures were different. The hardness increased slightly after electron irradiation, but the increase did not depend on the irradiation dose. If samples were obtained at higher irradiation doses (e.g. more than 10^{-2} dpa), we would be able to detect a dose dependence on the change in hardness. The

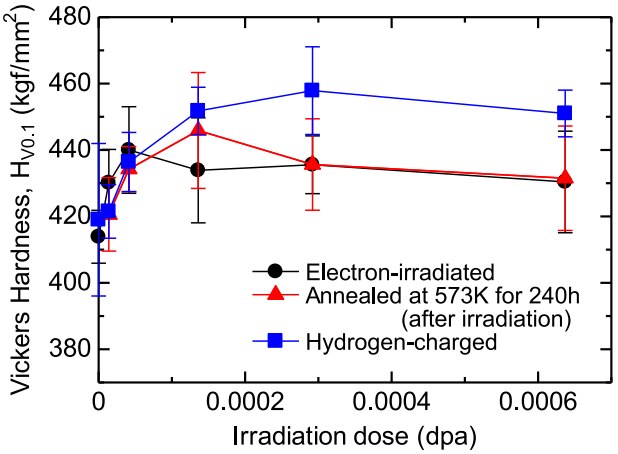

Fig. 5. Change in Vickers hardness of electron-irradiated tungsten versus irradiation dose.

hardness did not change after annealing at 573 K for 240 h except at a dose of 1.4×10^{-4} dpa. Sato et al. reported that interstitial clusters grew and single vacancies remained after a heat treatment using positron annihilation spectroscopy (PAS) [26]. However, this microstructural change did not affect the change in hardness. At a dose of 1.4×10^{-4} dpa, the hardness increased. The cause is not clear, and we need to clarify it in the future. After hydrogen charging, the hardness increased at doses greater than 1×10^{-4} dpa. This was because of the formation of single vacancies decorated with hydrogen atoms [26], which obstructed the motion of dislocations.

Fig. 7 shows the change in Vickers hardness of tungsten irradiated

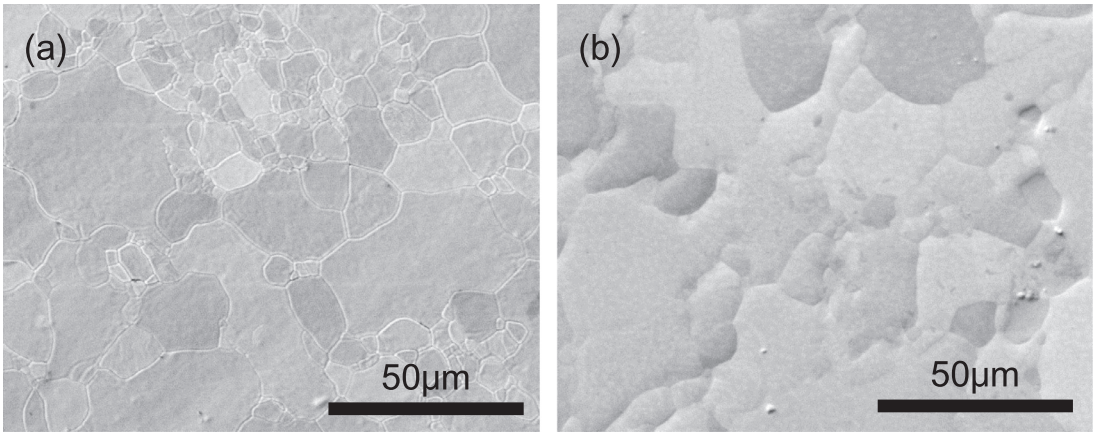

Fig. 6. SEM images of the surface of (a) tungsten annealed at 1773 K for 1 h used in Section 3.2 and (b) tungsten irradiated with electrons at doses of 6.4×10^{-5} dpa.

with electrons at doses of 6.4×10^{-5} dpa. The labels "e-irr.," "ann.," and "H.C." denote electron irradiation, annealing at 573 K for 240 h before hydrogen charging, and after hydrogen charging, respectively. The hardness increased after annealing at 323 K. Hydrogen atoms trapped at weak trapping sites (grain boundaries or dislocation loops) dissociate at 323 K and are captured at stronger trapping sites (irradiation-induced vacancies). The increase in the hardness at 323 K is due to this phenomenon, which was not obtained in PAS [26] because of the resolution of the PAS machine. The hardness greatly decreased after annealing at 473 K. In [26], Sato et al. reported that single vacancies captured one or two hydrogen atoms (an average of 1.6 atoms), and the hydrogen binding energy was 1.19 eV in their tungsten samples, the same as used in this study. During annealing at 423, 473, and 523 K for 1 h, the de-trapping frequencies of hydrogen atoms from single vacancies ($\nu_0 \exp(-(E_b + E_m)/k_B T)$, k_B: Boltzmann constant, T: absolute temperature) were factors of ~0.005, 0.5, and 21 using the hydrogen binding energy E_m of 1.19 eV, hydrogen migration energy E_m of 0.39 eV [27] and frequency factor ν_0 of 10^{13} /s, respectively. Half of the hydrogen atoms trapped at single vacancies were dissociated at an annealing temperature of 473 K after 1 h in the rough estimates mentioned above. The dissociation of hydrogen atoms from single vacancies led to a decrease in the hardness after annealing at 473 K. However, according to a molecular dynamics simulation, single vacancies decorated with hydrogen atoms cannot obstruct the dislocation motion in α-Fe [28]. To investigate this contradiction, a molecular dynamics simulation of tungsten should be performed. The dependence of the number of hydrogen atoms trapped at single vacancies on the increased hardness should also be examined. Terentyev et al. indicated that the formation of vacancy cluster-hydrogen isotope complexes induced by high flux plasma can lead an increase in the hardness [23]. If Terentyev et al. performed the isochronal annealing, the effect of hydrogen isotopes on the hardness of tungsten would be clarified.

4. Concluding remarks

Vickers hardness and tensile tests were conducted on electron-irradiated and stress-relieved tungsten to investigate the effect of hydrogen on the mechanical properties of tungsten. The following results were obtained in this study.

1. In as-received and stress-relieved tungsten, the Vickers hardness and tensile behavior prior to hydrogen charging at a pressure of 5.8 MPa were nearly the same as those after. Hydrogen atoms had no influence on dislocation motion due to low hydrogen solubility.
2. In electron-irradiated tungsten, after hydrogen charging, irradiation-induced single vacancies captured hydrogen atoms, and the Vickers hardness consequently increased.
3. After annealing the hydrogen-charged electron-irradiated tungsten

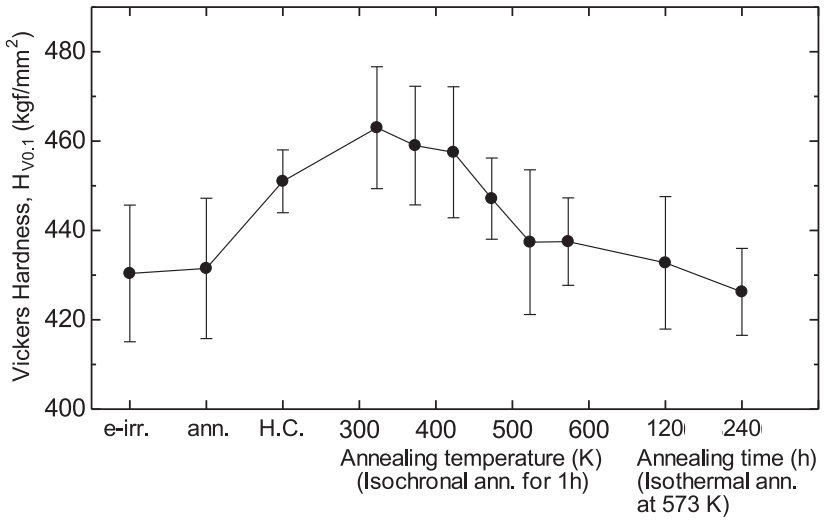

Fig. 7. Change in Vickers hardness of tungsten irradiated with electrons at doses of 6.4×10^{-5} dpa. The labels "e-irr.," "ann.," and "H.C." denote electron irradiation, annealing at 573 K for 240 h before hydrogen charging, and after hydrogen charging, respectively. These treatments were applied to one sample in sequence.

at 473 K, the hardness began to decrease because a sufficient amount of hydrogen atoms dissociated from single vacancies at 473 K.

This study obtained interesting results leading to the elucidation of hydrogen embrittlement in tungsten. However, additional simulations are needed to clarify the hardening mechanism triggered by single vacancies decorated with hydrogen atoms. The effect of the number of hydrogen atoms trapped at single vacancies on the hardness should also be investigated by higher pressure hydrogen charging, which will clarify the change in the mechanical properties caused by the interaction between hydrogen atoms and dislocations.

Acknowledgment

This work was supported by the "Joint Usage/Research Program on Zero-Emission Energy Research, Institute of Advanced Energy, Kyoto University (ZE29B-23)."

References

[1] Y. Hatano, M. Shimada, Y. Oya, G. Cao, M. Kobayashi, M. Hara, B.J. Merrill, K. Okuno, M.A. Sokolov, Y. Katoh, Mater. Trans. 54 (2013) 437.
[2] D. Terentyev, V. Dubinko, A. Bakaev, Y. Zayachuk, W. Van Renterghem, P. Grigorev, Nucl. Fusion 54 (2014) 042004.
[3] S. Kajita, S. Takamura, N. Ohno, D. Nihijima, H. Iwakiri, N. Yoshida, Nucl. Fusion 47 (2007) 1358.
[4] A. Loarte, G. Saibene, R. Sartori, M. Becoulet, L. Horton, T. Eich, A. Herrmann, M. Laux, G. Matthews, S. Jachmich, N. Asakura, A. Chankin, A. Leonard, G. Porter, G. Federici, M. Shimada, M. Sugihara, G. Janeschitz, J. Nucl. Mater. 313 (2003) 962.
[5] N. Noda, V. Philipps, R. Neu, J. Nucl. Mater. 241–243 (1997) 227.
[6] M. Rieth, S.L. Dudarev, S.M. Gonzalez de Vicente, J. Aktaa, T. Ahlgren, S. Antusch, D.E.J. Armstrong, M. Balden, N. Baluc, M.-F. Barthe, W.W. Basuki, M. Battabyal, C.S. Becquart, D. Blagoeva, H. Boldyryeva, J. Brinkmann, M. Celino, L. Ciupinski, J.B. Correia, A. De Backer, C. Domain, E. Gaganidze, C. García-Rosales, J. Gibson, M.R. Gilbert, S. Giusepponi, B. Gludovatz, H. Greuner, K. Heinola, T. Höschen, A. Hoffmann, N. Holstein, F. Koch, W. Krauss, H. Li, S. Lindig, J. Linke, Ch. Linsmeier, P. López-Ruiz, H. Maier, J. Matejicek, T.P. Mishra, M. Muhammed, A. Muñoz, M. Muzyk, K. Nordlund, D. Nguyen-Manh, J. Opschoor, N. Ordás, T. Palacios, G. Pintsuk, R. Pippan, J. Reiser, J. Riesch, S.G. Roberts, L. Romaner, M. Rosinski, M. Sanchez, W. Schulmeyer, H. Traxler, A. Ureña, J.G. van der Laan, L. Veleva, S. Wahlberg, M. Walter, T. Weber, T. Weitkamp, S. Wurster, M.A. Yar, J.H. You, A. Zivelonghi, J. Nucl. Mater. 432 (2013) 482.
[7] M. Shimada, Y. Hatano, P. Calderoni, T. Oda, Y. Oya, M. Sokolov, K. Zhang, G. Cao, R. Kolasinski, J.P. Sharpe, J. Nucl. Mater. 415 (2011) S667.
[8] N. Yoshida, J. Nucl. Mater. 266–269 (1999) 197.
[9] M. Tokitani, M. Miyamoto, K. Tokunaga, T. Fujiwara, N. Yoshida, S. Masuzaki, N. Ashikawa, T. Morisaki, M. Shoji, A. Komori, LHD Experimental Group, S. Nagata, B. Tsuchiya, J. Nucl. Mater. 363–365 (2007) 443.
[10] V.Kh. Alimov, J. Roth, R.A. Causey, D.A. Komarov, Ch. Lismeier, A. Wiltner, F. Kost, S. Lindig, J. Nucl. Mater. 375 (2008) 192.
[11] K. Ohsawa, J. Goto, M. Yamakami, M. Yamaguchi, M. Yagi, Phys. Rev. B 82 (2010) 184117.
[12] O.V. Ogorodnikova, J. Roth, M. Mayer, J. Nucl. Mater. 313–316 (2003) 469.
[13] O.V. Ogorodnikova, J. Roth, M. Mayer, J. Appl. Phys. 103 (2008) 034902.
[14] O.V. Ogorodnikova, J. Roth, M. Mayer, J. Nucl. Mater. 373 (2008) 254.
[15] R.A. Causey, T.J. Venhaus, Phys. Script. T94 (2001) 9.
[16] O.V. Ogorodnikova, T. Tyburska, V.Kh. Alimov, K. Ertl, J. Nucl. Mater. 415 (2011) S661.
[17] H.K. Birnbaum, P. Sofronis, Mater. Sci. Eng. A 176 (1994) 191.
[18] M. Nagumo, M. Nakamura, K. Takai, Metall. Mater. Trans. A 32 (2001) 339.
[19] H.K. Birnbaum, P. Sofronis, Mater. Sci. Eng. A 176 (1994) 191.
[20] R.A. Oriani, H. Josephic, Acta Metall 22 (1974) 1065.
[21] M. Nagumo, M. Nakamura, K. Takai, Metall. Mater. Trans. A 32 (2001) 339.
[22] X.G. Yu, F.J. Guo, X. Tian, J. Nucl. Mater. 441 (2013) 324.
[23] D. Terentyev, A. Bakaeva, T. Pardoen, A. Favache, E.E. Zhurkin, J. Nucl. Mater. 476 (2016) 1.
[24] K. Sato, R. Tamiya, Q. Xu, H. Tsuchida, T. Yoshiie, Nucl. Mater. Ene. 9 (2016) 554.
[25] F.F. Schmidt, H.R. Ogden, The Engineering Properties of Tungsten and Tungsten alloys, Defense Metals Information Center, Battelle Memorial Institute, Columbus, Ohio, 1963.
[26] K. Sato, A. Hirosako, K. Ishibashi, Y. Miura, Q. Xu, M. Onoue, Y. Fukutoku, T. Onitsuka, M. Hatakeyama, S. Sunada, T. Yoshiie, J. Nucl. Mater. 496 (2017) 9.
[27] R. Frauenfelder, J. Vac. Sci. Technol. 6 (1969) 388.
[28] S.Z. Li, Y.G. Li, Y.C. Lo, T. Neeraj, R. Srinivasan, X.D. Ding, J. Sun, L. Qi, P. Gumbsch, J. Li, Int. J. Plasticity 74 (2015) 175.